Table 2
Comparison of mean threshold cycle (C_T) of genes used in the present study in the methacarn-fixed paraffin-embedded rat liver tissue by real-time RT-PCR[a]

Tissue condition	No. of samples	Genes			
		GAPDH[b]	CYP2B1[b]	Slc34a2[c]	Stx6[c]
Fixation/dehydration[d]					
2 h/overnight	3	16.7	13.2	26.4	27.3
Temperature/duration of storage[e]					
4 °C/1 month	6	16.5	13.1	24.7	27.5

[a] Liver of a rat treated with PB for 3 days was used. C_T values in the 50 ng total RNA were measured at the fixed fluorescence threshold level of 0.14.
[b] Signal detection was performed by one-step real-time RT-PCR with the SYBR Green detection system.
[c] Signal detection was performed by two-step real-time RT-PCR with the TaqMan probe detection system.
[d] Examination of the effect of time length for tissue processing (Experiment 1). Already prepared PETs were stored at 4 °C until all of the tissues were processed for embedding.
[e] Examination of the effect of tissue storage with regard to the period and its temperature (Experiment 2). At the end of storage, tissue sections were prepared and stored at −80 °C until analysis.

of GAPDH, slc34a2, and stx6, to 76.1, 54.6, and 44.5%, respectively, of that for 1 month storage at 4 °C (Fig. 3B). Other storage conditions did not apparently affect the retention of mRNAs, while nonsignificant reduction was noted with slc34a2 stored for 3 months at 4 °C. CV values were mostly within 20%, except for those of slc34a2, ranging 21.3–33.8.

Integrity and yield of polypeptides

In Experiment 1, the visual pattern of resolved polypeptide bands and their intensities in polyacrylamide gels did not differ among samples with the tissue-processing conditions (Fig. 4A). However, protein yield was reduced in the 1-week dehydrated case as compared with that in the overnight dehydrated case after 2-h fixation (Fig. 5A).

In Experiment 2, the visual patterns of polypeptide bands were similar under the different storage conditions, but their intensities were rather reduced in the case of storage for 12 months at room temperature (Fig. 4B). With regard to protein yield, this was slightly reduced with storage of PETs at room temperature, reaching statistical significance in the 3-month storage case (Fig. 5B).

Levels of protein signals retained in PETs

In Experiment 1, retained levels of β-actin did not differ between the 2-h-fixed/overnight-dehydrated and other fixation/dehydration conditions, and variability in each was rather small (CV values <20%) (Fig. 6A). With PCNA, increase of relative expression was observed in samples fixed for 2 h and kept for 1 week at the dehydration step, the level being 132% of that with overnight dehydration, but the CV value was rather small (<20%) irrespective of the tissue-processing condition. In the EGFR case, a tendency for reduction of relative expression level was observed in 1-week-dehydrated PETs as compared with similar fixation for 2 h but dehydration overnight. However, this was not significant at least partly due to the variability in the expression values among samples in each condition, with CV values ranging 24.2–34.5%.

In Experiment 2, the retained expression level of β-actin was reduced in PETs stored at room temperature for more than 3 months, to 74% at 3 months and 52% at 12 months of the 1-month value at 4 °C (Fig. 6B). Slight, insignificant

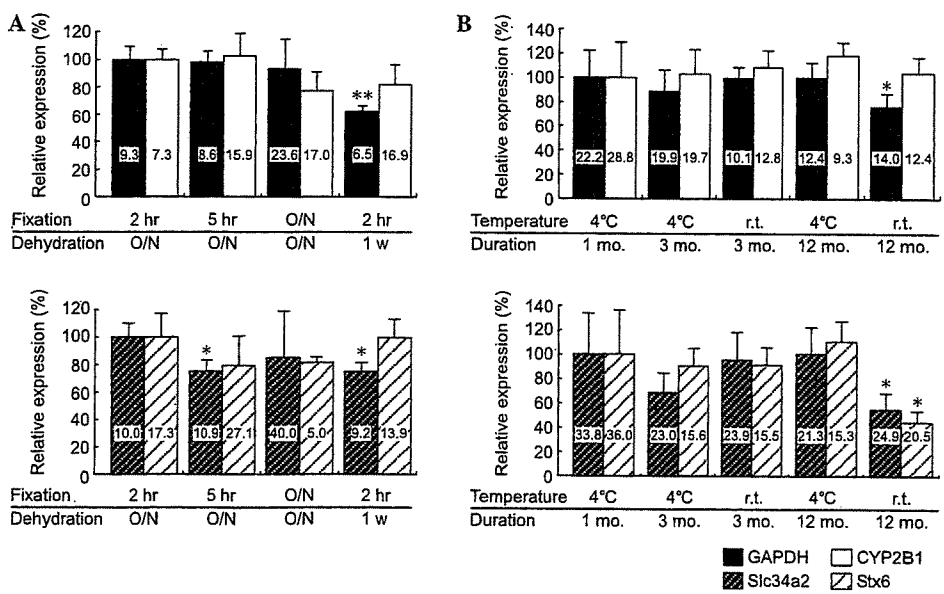

Fig. 3. Relative expression levels of GAPDH, CYP2B1, slc34a2, and stx6 mRNAs in methacarn-fixed PETs under the different conditions of tissue processing or storage. GAPDH and CYP2B1 mRNA levels were measured by one-step real-time RT-PCR with the SYBR Green detection system, and slc34a2 and stx6 mRNA levels were measured by two-step real-time RT-PCR with the TaqMan probe detection system. (A) Experiment 1 ($n = 3$ for each condition). (B) Experiment 2 ($n = 6$ for each condition). Data are mean ± SD values and coefficients of variation (CVs). *, **Significantly different from the 2-h-fixed/overnight-dehydrated case in Experiment 1, or from the 1-month-storage case at 4 °C in Experiment 2 ($^*p < 0.05$, $^{**}p < 0.01$).

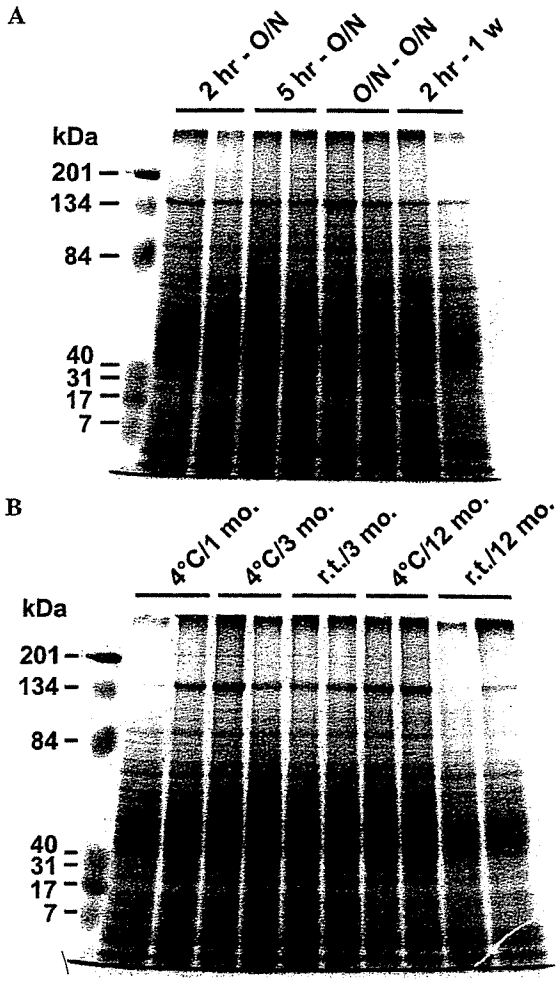

Fig. 4. Integrity of polypeptide bands in protein extracts from methacarn-fixed PETs under different conditions of tissue processing or storage. (A) Experiment 1. (B) Experiment 2.

reduction in the β-actin level was also evident in samples stored for 12 months at 4 °C, but here variability among storage conditions was relatively small, except for the case at room temperature for 12 months, with the CV value of 30.8%. With PCNA, no apparent reduction in protein signals was observed irrespective of the storage condition. For EGFR, a tendency for decrease was observed in samples stored for 3 months at room temperature and 12 months at 4 °C. Storage at room temperature for 12 months was associated with a level only 28% of the value for 1 month at 4 °C.

Discussion

Usually, formaldehyde-based cross-linking agents, such as buffered formalin, limit molecular analysis of DNAs, RNAs, and proteins due to direct interactions with these biomolecules [14]. However, in addition to methacarn, several alternative noncross-linking fixatives, such as HOPE solution [15–17], zinc-based agents [18], acetone-based AMeX [19], and alcohol or alcohol-based fixatives [20,21], have been developed for better preservation of nucleic acids and proteins in PETs. However, information on the effects of tissue processing and storage has hitherto been limited. We here revealed that fixation for a period up to overnight did not affect either the integrity or the expression levels of RNAs and proteins. On the other hand, dehydrating tissues for 1 week did result in slight fluctuations in the relative expression level of both molecular species. Integrity of both total RNAs and polypeptides was retained with storage of PETs at 4 °C but was reduced at room temperature over 12 months. Reflecting the reduction in the integrity, levels of molecules retained after storage at room temperature were also reduced. Reduction was apparent in protein levels by storage for more than 3 months, while this was evident in mRNA levels by 12 months storage.

With regard to the fixation condition in Experiment 1 of the present study, fixation for 5 h resulted in slight reduction in the slc34a2 mRNA level. Although statistical significance was not attained, a similar weak reduction was also noted on another minor mRNA species stx6. However, these reductions lacked apparent time dependency, showing no further reduction by overnight fixation. On the other hand, although most data have not been quantitatively measured and statistically analyzed, tissue fixation with a universal molecular fixative (UMFIX), composed of methanol and polyethylene glycol at a predetermined ratio (Sakura Finetek USA, Inc., Torrance, CA), for 24 h resulted in no obvious changes in either the integrity of extracted total

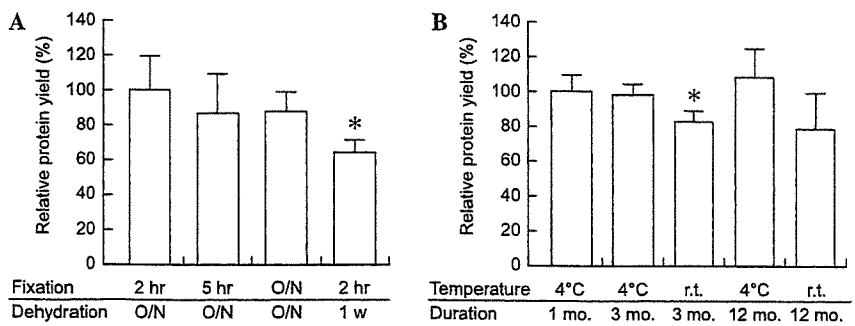

Fig. 5. Relative protein yields from methacarn-fixed PETs under different conditions for tissue processing or storage. (A) Experiment 1 ($n = 3$ for each condition). (B) Experiment 2 ($n = 3$ for each condition). Data are mean ± SD values. *Significantly different from the 2-h-fixed/overnight-dehydrated case in Experiment 1 or from the 1-month-storage case at 4 °C in Experiment 2 ($*p < 0.05$).

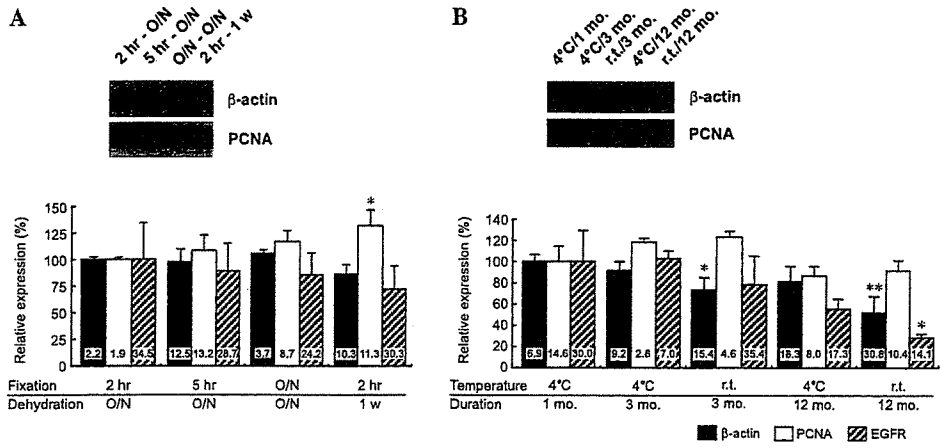

Fig. 6. Relative expression levels of β-actin, PCNA, and EGFR in methacarn-fixed PETs under different conditions of tissue processing or storage. (A) Experiment 1 ($n = 3$ for each condition). (B) Experiment 2 ($n = 3$ for each condition). Data are mean ± SD values and coefficients of variations (CVs). Each inset shows representative blot data for β-actin and PCNA. *, **Significantly different from the 2-h-fixed/overnight-dehydrated case in Experiment 1 or from the 1-month-storage case at 4 °C in Experiment 2 ($^{*}p < 0.05$, $^{**}p < 0.01$).

RNAs or the C_T for detection of GAPDH mRNA levels on real-time RT-PCR analysis, despite slight deterioration of protein signals being evident as compared with the 1-h-fixed case [21]. Taking all the results in combination, fixation with alcohol-based fixatives for more than 24 h may affect protein expression levels, but the effect on mRNA expression may be marginal.

Our findings for dehydration suggest the possibility of release of protein molecules into ethanol solution over time, although levels of nuclear protein PCNA and membrane-bound EGFR were increased (significant) and decreased (nonsignificant), respectively. Lipid extraction by alcohol-based protein precipitating fixatives may result in diffusion artifacts of membrane-bound proteins, causing difficulties with their immunohistochemical detection [22–24]. In our previous study, slight loss of protein yield in methacarn-fixed PETs as compared with UFTs was suggestive of diffusion artifacts [5]. While we observed high variability of EGFR levels among samples as compared with those for PCNA and cytoskeletal β-actin in Experiment 1, this was irrespective of the period of fixation and dehydration. One-week dehydration here also resulted in relative decrease of the mRNA levels of GAPDH and slc34a2, although diffusion artifacts may not have played a role because (i) the yield of total RNA was equivalent to that with other tissue-processing conditions and (ii) the mRNA expression of other genes, CYP2B1 and stx6, was not altered.

With regard to tissue storage effects, RNA degradation was evident in the study using UMFIX-fixed PETs from the visual pattern of major isoforms of ribosomal RNAs, and the cDNA array profile was changed by storage for 4 or 8 weeks at room temperature [21], although the authors argued that the extracted total RNAs were nondegraded and the cDNA array profile was comparable with results for freshly prepared PETs. In the present study, both 18S and 28S ribosomal RNAs mostly disappeared in methacarn-fixed PETs stored for 12 months at room temperature, suggesting degradation over time. On the other hand, mRNA levels in these samples were not entirely affected on measurement with real-time RT-PCR. Usually, real-time PCR utilizes target fragments sized only around 100 bp, and therefore not all RNA molecules in methacarn-fixed PETs are lost on long-term storage at room temperature. Interestingly, this reduction was apparent in mRNA species with low copy numbers, suggesting an uneven effect of long-term storage on degradation of mRNA species, although the corresponding mechanism was unclear.

Integrity of both total RNAs and proteins was well preserved at 4 °C in our study, in accordance with a previous report for the AMeX method, in which only minimal degradation of polypeptides resolved on polyacrylamide gels was documented for a period of 2 years at 4 °C [19]. On the other hand, as with total RNA, decreased intensity of polypeptides in gels was observed with our methacarn-fixed PETs stored for 12 months at room temperature, paralleling the reduced expression levels noted for two of three proteins examined. Oxidation of tissue samples during storage may cause modification of nucleic acids and proteins to affect their yield and integrity [14,25]. In the case of sectioned tissue samples, under ambient conditions they rapidly lose antigenicity; however, the magnitude of this loss differs from antigen to antigen [25]. Variation in the retained expression levels of our three proteins might reflect a similar phenomenon. For tissue sections, combined nitrogen storage and paraffin coating is a useful technique for preserving antigenicity [25]. With regard to storage of PETs, use of vacuum packing is recommended for prevention of oxidation [14]. In the context of tissue storage for future research purposes, vacuum packing may similarly be warranted.

In summary, for gene expression analysis using methacarn-fixed PETs, tissues can be fixed overnight. Moreover, considering similar expression variability among processing conditions, fixed tissues can be kept at the dehydration step for at least 1 week, and PETs can be stored for at least 12 months, but preferably at a temperature of 4 °C in a refrigerator.

Acknowledgments

Dr. Lee was an Awardee of a Postdoctoral Fellowship Program from the Japan Society for the Promotion of Science during the performance of this study. This work was supported by Health and Labour Sciences Research Grants (Risk Analysis Research on Food and Pharmaceuticals) from the Ministry of Health, Labour and Welfare of Japan.

References

[1] M.R. Emmert-Buck, R.F. Bonner, P.D. Smith, R.F. Chuaqui, Z. Zhuang, S.R. Goldstein, R.A. Weiss, L.A. Liotta, Laser capture microdissection, Science 274 (1996) 998–1001.

[2] K. Schütze, G. Lahr, Identification of expressed genes by laser-mediated manipulation of single cells, Nat. Biotechol. 16 (1998) 737–742.

[3] M. Harsch, K. Bendrat, G. Hofmeier, D. Branscheid, A. Niendorf, A new method for histological microdissection utilizing an ultrasonically oscillating needle: demonstrated by differential mRNA expression in human lung carcinoma tissue, Am. J. Pathol. 158 (2001) 1985–1990.

[4] H. Puchtler, F.S. Waldrop, S.N. Meloan, M.S. Terry, H.M. Conner, Methacarn (Methanol-Carnoy) fixation. Practical and theoretical considerations, Histochemie 21 (1970) 97–116.

[5] M. Shibutani, C. Uneyama, K. Miyazaki, K. Toyoda, M. Hirose, Methacarn fixation: a novel tool for analysis of gene expressions in paraffin-embedded tissue specimens, Lab. Invest. 80 (2000) 199–208.

[6] C. Uneyama, M. Shibutani, K. Nakagawa, N. Masutomi, M. Hirose, Methacarn, a fixation tool for multipurpose gene expression analysis from paraffin-embedded tissue materials, Curr. Topics Biochem. Res. 3 (2000) 237–242.

[7] M. Shibutani, C. Uneyama, Methacarn: a fixation tool for multipurpose genetic analysis from paraffin-embedded tissues, in: P.M. Conn (Ed.), Laser Capture Microscopy and Microdissection, Methods Enzymol, vol. 356, Academic Press, London, 2002, pp. 114–125.

[8] C. Uneyama, M. Shibutani, N. Masutomi, H. Takagi, M. Hirose, Methacarn fixation for genomic DNA analysis in microdissected, paraffin-embedded tissue specimens, J. Histochem. Cytochem. 50 (2002) 1237–1245.

[9] H. Takagi, M. Shibutani, N. Kato, H. Fujita, K.-Y. Lee, S. Takigami, K. Mitsumori, M. Hirose, Microdissected region-specific gene expression analysis with methacarn-fixed paraffin-embedded tissues by real-time RT-PCR, J. Histochem. Cytochem. 52 (2004) 903–913.

[10] M. Shibutani, C. Uneyama, Methacarn fixation for genomic DNA analysis in microdissected cells, in: G.I. Murray, S. Curran (Eds.), Laser Capture Microdissection and its Applications, Humana Press, Totowa, Methods Mol. Biol. 293 (2004) 11–25.

[11] J.O. Kim, H.N. Kim, M.H. Hwang, H.I. Shin, S.Y. Kim, R.W. Park, E.Y. Park, I.S. Kim, A.J. van Wijnen, J.L. Stein, J.B. Lian, G.S. Stein, J.Y. Choi, Differential gene expression analysis using paraffin-embedded tissues after laser microdissection, J. Cell. Biochem. 90 (2003) 998–1006.

[12] T.A. Kocarek, J.M. Kraniak, A.B. Reddy, Regulation of rat hepatic cytochrome P450 expression by sterol biosynthesis inhibition: inhibitors of squalene synthase are potent inducers of CYP2B expression in primary cultured rat hepatocytes and rat liver, Mol. Pharmacol. 54 (1998) 474–484.

[13] T.D. Schmittgen, B.A. Zakrajsek, A.G. Mills, V. Gorn, M.J. Singer, M.W. Reed, Quantitative reverse transcription-polymerase chain reaction to study mRNA decay: comparison of endpoint and real-time methods, Anal. Biochem. 285 (2000) 194–204.

[14] M. Srinivasan, D. Sedmak, S. Jewell, Effect of fixatives and tissue processing on the content and integrity of nucleic acids, Am. J. Pathol. 161 (2002) 1961–1971.

[15] J. Olert, K.H. Wiedorn, T. Goldmann, H. Kühl, Y. Mehraein, H. Scherthan, F. Niketeghad, E. Vollmer, A.M. Müller, J. Müller-Navia, HOPE fixation: a novel fixing method and paraffin-embedding technique for human soft tissues, Pathol. Res. Pract. 197 (2001) 823–826.

[16] K.H. Wiedorn, J. Olert, R.A. Stacy, T. Goldmann, H. Kühl, J. Matthus, E. Vollmer, A. Bosse, HOPE—a new fixing technique enables preservation and extraction of high molecular weight DNA and RNA of >20 kb from paraffin-embedded tissues. Hepes–glutamic acid buffer mediated organic solvent protection effect, Pathol. Res. Pract. 198 (2002) 735–740.

[17] U. Uhlig, S. Uhlig, D. Branscheid, P. Zabel, E. Vollmer, T. Goldmann, HOPE technique enables Western blot analysis from paraffin-embedded tissues, Pathol. Res. Pract. 200 (2004) 469–472.

[18] K. Wester, A. Asplund, H. Bäckvall, P. Micke, A. Derveniece, I. Hartmane, P.U. Malmström, F. Pontén, Zinc-based fixative improves preservation of genomic DNA and proteins in histoprocessing of human tissues, Lab. Invest. 83 (2003) 889–899.

[19] Y. Sato, K. Mukai, S. Furuya, T. Kameya, S. Hirohashi, The AMeX method: a multipurpose tissue-processing and paraffin-embedding method. Extraction of protein and application to immunoblotting, Am. J. Pathol. 140 (1992) 775–779.

[20] J.W. Gillespie, C.J. Best, V.E. Bichsel, K.A. Cole, S.F. Greenhut, S.M. Hewitt, M. Ahram, Y.B. Gathright, M.J. Merino, R.L. Strausberg, J.I. Epstein, S.R. Hamilton, G. Gannot, G.V. Baibakova, V.S. Calvert, M.J. Flaig, R.F. Chuaqui, J.C. Herring, J. Pfeifer, E.F. Petricoin, W.M. Linehan, P.H. Duray, G.S. Bova, M.R. Emmert-Buck, Evaluation of non-formalin tissue fixation for molecular profiling studies, Am. J. Pathol. 160 (2002) 449–457.

[21] V. Vincek, M. Nassiri, M. Nadji, A.R. Morales, A tissue fixative that protects macromolecules (DNA, RNA, and protein) and histomorphology in clinical samples, Lab. Invest. 83 (2003) 1427–1435.

[22] B. Gusterson, G. Cowley, J.A. Smith, B. Ozanne, Cellular localisation of human epidermal growth factor receptor, Cell Biol. Int. Rep. 8 (1984) 649–658.

[23] M.A. Judd, K.J. Britten, Tissue preparation for the demonstration of surface antigens by immunoperoxidase techniques, Histochem. J. 14 (1982) 747–753.

[24] B.A. Ponder, M.M. Wilkinson, Inhibition of endogenous tissue alkaline phosphatase with the use of alkaline phosphatase conjugates in immunohistochemistry, J. Histochem. Cytochem. 29 (1981) 981–984.

[25] K.A. DiVito, L.A. Charette, D.L. Rimm, R.L. Camp, Long-term preservation of antigenicity on tissue microarrays, Lab. Invest. 84 (2004) 1071–1078.

Hypothalamus Region-Specific Global Gene Expression Profiling in Early Stages of Central Endocrine Disruption in Rat Neonates Injected with Estradiol Benzoate or Flutamide

Makoto Shibutani,[1] Kyoung-Youl Lee,[1]* Katsuhide Igarashi,[2] Gye-Hyeong Woo,[1] Kaoru Inoue,[1] Tetsuji Nishimura,[3] Masao Hirose[1]

WILEY InterScience® DISCOVER SOMETHING GREAT

Hypothalamus Region-Specific Global Gene Expression Profiling in Early Stages of Central Endocrine Disruption in Rat Neonates Injected with Estradiol Benzoate or Flutamide

Makoto Shibutani,[1] Kyoung-Youl Lee,[1]* Katsuhide Igarashi,[2] Gye-Hyeong Woo,[1] Kaoru Inoue,[1] Tetsuji Nishimura,[3] Masao Hirose[1]

[1] Division of Pathology, National Institute of Health Sciences, Setagaya-ku, Tokyo 158-8501, Japan

[2] Division of Molecular Toxicology, National Institute of Health Sciences, Setagaya-ku, Tokyo 158-8501, Japan

[3] Division of Environmental Chemistry, National Institute of Health Sciences, Setagaya-ku, Tokyo 158-8501, Japan

Received 3 February 2006; revised 8 September 2006; accepted 14 September 2006

ABSTRACT: **To identify genes linked to early stages of disruption of brain sexual differentiation, hypothalamic region-specific microarray analyses were performed using a microdissection technique with neonatal rats exposed to endocrine-acting drugs. To validate the methodology, the expression fidelity of microarrays was first examined with two-round amplified antisense RNAs (aRNAs) from methacarn-fixed paraffin-embedded tissue (PET) in comparison with expression in unfixed frozen tissue (UFT). Decline of expression fidelity when compared with the 1×-amplified aRNAs from UFTs was found as a result of the preferential amplification of the 3′ side of mRNAs in the second round *in vitro* transcription. However, expression patterns for the 2×-amplified aRNAs were mostly identical between methacarn-fixed PET and UFT, suggesting no obvious influence of methacarn fixation and subsequent paraffin embedding on expression levels. Next, in the main experiment, neonatal rats at birth were treated subcutaneously either with estradiol benzoate (EB; 10 μg/pup) or flutamide (FA; 250 μg/pup), and medial preoptic area (MPOA)-specific microarray analysis was performed 24 h later using 2×-amplified aRNAs from methacarn-fixed PET. Numbers of genes showing constitutively high expression in the MPOA predominated in males, implying a link with male-type growth supported by perinatal testosterone. Around 60% of genes showing sex differences in expression demonstrated altered levels after EB treatment in females, suggesting an involvement of genes necessary for brain sexual differentiation. When compared with EB, FA affected a rather small number of genes, but fluctuation was mostly observed in females, as with EB. Moreover, many selected genes common to EB and FA showed down-regulation in females with both drugs, suggesting a common mechanism for endocrine center disruption in females, at least at early stages of post-natal development.** © 2007 Wiley Periodicals, Inc. Develop Neurobiol 67: 253–269, 2007

Keywords: **brain sexual differentiation; microarray; estradiol benzoate; flutamide; microdissection**

INTRODUCTION

Sex steroids play important roles in sexual differentiation of the mammalian brain (McEwen and Alves, 1999). In the rat, there is a critical period beginning

**Present address:* Toxicological Research Team, Occupational Safety and Health Research Institute, 104-8, Munji-Dong, Yuseong-Gu, Daejeon, 305-380, Korea.

Correspondence to: M. Shibutani (shibutan@nihs.go.jp).

Contract grant sponsors: Ministry of the Environment, Ministry of Health, Labor and Welfare of Japan.

© 2007 Wiley Periodicals, Inc.

Published online 3 January 2007 in Wiley InterScience (www.interscience.wiley.com).
DOI 10.1002/dneu.20349

at the last week of gestation and terminating in few days after birth, during which circulating testosterone secreted from the fetal and neonatal testes masculinizes the brain in males (Rhees et al., 1990a,b), the hormone being metabolized to estradiol by the enzyme aromatase to trigger brain sexual differentiation. Steroid-mediated processes during this period, including alterations in neuronal plasticity, myelination, and cell death, are the basis of sexual dimorphism in the structure and function of the adult brain (Matsumoto et al., 2000). For example, the medial preoptic area (MPOA) in the hypothalamus that is believed to mediate sexually dimorphic behavior in adult life (Meisel and Sachs, 1994; Numan, 1994) contains a highly cellular region, the sexually dimorphic nucleus of preoptic area (SDN-POA), that has an approximately 10 times larger volume in males than in females (Meredith et al., 2001). Inhibitory effects of steroids against the normal apoptosis that proceeds in the female SDN-POA during the critical period have been suggested to be responsible for the large size in males (Arai et al., 1996; Davis et al., 1996).

Sex steroids with their receptors are powerful regulators of gene transcription, and changes in the hormonal milieu during development can trigger reproductive dysfunction in later life by affecting molecular cascades responsible for sexual differentiation (McEwen and Alves, 1999). For instance, both α and β estrogen receptors (ERs) are strongly expressed in the hypothalamus during neonatal development, showing region-specific distributions (Orikasa et al., 2002), and neonatal hormonal manipulations can affect their expression levels and/or locations (Tena-Sempere et al., 2001; Orikasa et al., 2002), resulting in organizational changes in the brain structure and reproductive function in later life (Nagao et al., 1999; Tsukahara et al., 2003).

To elucidate mechanisms underlying disruption of brain sexual differentiation, gene screening applying global gene expression profiling in target brain region(s) is an effective approach. We recently established multipurpose genetic analysis methods with paraffin-embedded tissues (PETs) utilizing methacarn as a novel fixation tool, in combination with laser microbeam microdissection (Shibutani et al., 2000; Shibutani and Uneyama, 2002; Uneyama et al., 2002). With this system, we could achieve high performance regarding quantitative expression analysis of mRNAs using real-time RT-PCR, close to that with unfixed frozen tissue (UFT) (Takagi et al., 2004).

In the present study, we focused on region-specific gene expression analysis utilizing microarrays to identify genes linked with disruption of brain sexual differentiation in rats. With limited tissue samples, such as those collected by microdissection, multi-round amplification of mRNAs is necessary to obtain sufficient quantities of antisense RNAs (aRNAs) applicable for microarray analysis, and therefore, we first performed validation experiments using methacarn-fixed liver PETs to determine fidelity of expression profiles with 2× *in vitro* transcribed aRNAs in comparison with 1×- or 2×-amplified examples from UFTs. After confirmation of the efficacy of the methods, we then analyzed gene expression profiles in the neonatal MPOA in terms of sex differences and acute responses to neonatally injected estradiol benzoate (EB), a potent analog of endogenous estrogen, or flutamide (FA), a non-steroidal anti-androgen.

METHODS

Chemicals and Animals

Estradiol benzoate (EB; CAS# 50-50-0) and flutamide (FA; CAS# 13311-84-7) were purchased from Sigma (St. Louis, MO), sodium phenobarbital (PB; CAS# 57-30-7) from Wako Pure Chemical Industries (Osaka, Japan) and CD®(SD)IGS rats from Charles River Japan (Kanagawa, Japan). For the preliminary validation study regarding expression fidelity with microarrays using methacarn-fixed PET, one 7-week-old male rat was used, and for gene expression profiling in the early stage of disruption of brain sexual differentiation, six pregnant rats at gestational Day 3 (the day when vaginal plugs were observed was designated as GD 0). The animals were housed individually in polycarbonate cages (SK-Clean, 41.5 × 26 × 17.5 cm in size; CLEA Japan, Tokyo) with wood bedding (Soft Chip; Sankyo Lab Service, Tokyo, Japan), maintained in an air-conditioned animal room (temperature: 24°C ± 1°C, relative humidity: 55% ± 5%) with a 12-h light–dark cycle, and allowed *ad libitum* access to feed and tap water. For the rat in the preliminary validation study, CRF-1, a standard rodent diet, purchased from Oriental Yeast Co. (Tokyo, Japan), was used as the basal diet. For pregnant animals, soy-free diet (Oriental Yeast Co.) was used as a basal diet to remove possible interaction of phytoestrogens included in the regular soy-containing diet with the action of EB or FA. The formulation of the soy-free diet as well as the dietary concentrations of estrogens and phytoestrogens were as described earlier (Masutomi et al., 2003). Essentially, concentrations of phytoestrogens except for coumestrol, detected at 0.3 mg/100 g diet, were lower than the detection limit (0.05 mg/100 g diet).

Experimental Design

In the preliminary validation study, the rat received PB intraperitoneally at 80 mg/kg, once daily for three days. The dose was selected according to the PB-specific enzyme

induction protocol described by Kocarek et al. (1998). One day after the last injection, the animal was killed by exsanguination from the abdominal aorta under ether anesthesia, and the liver was removed and trimmed to make tissue blocks sized 5 × 5 × 3 mm.

For gene expression profiling in the early stage of disruption of brain sexual differentiation, offspring of two dams each were injected subcutaneously either with EB, FA, or vehicle at postnatal day (PND) 1 (the day of delivery) within 3–6 h after completion of delivery. The dose level of EB was set as 10 μg/pup, shown in our laboratory, to induce typical estrogenic effects on sexual development and the endocrine/reproductive system at the adult stage in both sexes, including reduction of the SDN volume in males (Shibutani et al., 2005). For FA, 250 μg/pup was selected on the basis of earlier study finding of retardation of male reproductive development with repeated injections of this dose (Rivas et al., 2002). Each chemical was dissolved in sesame oil to achieve a total injection volume of 20 μL. Vehicle control animals were injected with 20 μL of sesame oil. Twenty-four hours after the injection (PND 2), offspring including vehicle control pups were killed by decapitation for removal of brains.

The animal protocols were reviewed and approved by the Animal Care and Use Committee of the National Institute of Health Sciences, Japan.

Preparation of Tissue Specimens and Microdissection

Liver tissues of the rat treated with PB were either quick frozen in ethanol–dry ice after embedding in Tissue-Tek 4583 OCT compound (Sakura Finetek Japan, Tokyo, Japan), or immersed in methacarn for tissue fixation. For this purpose, methacarn solution consisting of 60% (vol/vol) absolute methanol, 30% chloroform, and 10% glacial acetic acid was freshly prepared and stored at 4°C (Shibutani et al., 2000; Shibutani and Uneyama, 2002; Takagi et al., 2004), before fixation for 2 h at 4°C. Fixed tissue samples were then dehydrated three times for 1 h in fresh 99.5% ethanol at 4°C, immersed in xylene once for 1 h and then three times for 30 min at room temperature, and immersed in hot paraffin (60°C) four times for 1 h, for a total of 4 h. Both UFTs (n = 3) and methacarn-fixed PETs (n = 3) were sectioned at 10 μm and 20 sections per block were stored in 1.5 mL tubes at −80°C until RNA extraction.

For MPOA-specific microarray analysis, whole brains of rat pups were subjected to methacarn fixation (n = 3/sex/group). Before embedding, coronal brain slices including the hypothalamus were trimmed. Microdissection of the MPOA was performed based on the method described earlier (Takagi et al., 2004). After paraffin embedding, 6-μm-thick sections between three 18-μm-thick sections were prepared. The 18-μm sections were mounted onto PEN-foil film (Leica Microsystems, Tokyo, Japan) overlaid on glass slides, dried in an incubator overnight at 37°C, deparaffinized with xylene three times each for 3 min, placed in 99.5% ethanol for 1 min, and then air-dried. The localization of the SDN-POA, identified as an intensely stained cellular region, was determined by microscopic observation of the 6-μm-thick sections stained with hematoxylin and eosin (HE) (as shown in Fig. 1), and bilateral portions of the MPOA (500 × 300 μm) containing SDN-POA were microdissected from the adjacent unstained 18-μm-thick sections using PALM Robot-MicroBeam equipment (Carl Zeiss Co., Tokyo, Japan). In both sexes, 10–12 sections from one animal were used for microdissection, and the microdissected samples were stored in one 1.5 mL sample tube at −80°C until extraction of total RNA.

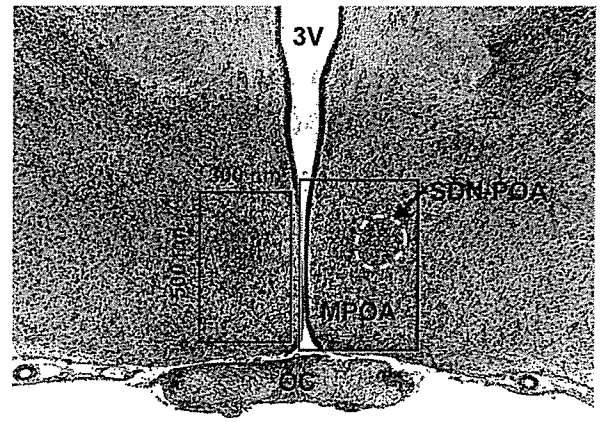

Figure 1 Overview of the hypothalamic MPOA at PND 2. Bilateral portions of MPOA as shown in the left boxed area were microdissected from sections of methacarn-fixed paraffin-embedded brain slices for gene expression analysis. The right boxed area is the anatomical location for immunohistochemical observation of protein signals shown in Table 6 and Fig. 6 (3V, third ventricle; SDN-POA, sexually dimorphic nucleus of the preoptic area; MPOA, medial preoptic area; OC, optic chiasm).

RNA Isolation, Amplification, and Microarray Analysis

Total RNAs from liver sections of UFTs and methacarn-fixed PETs were extracted with RNeasy® Mini (QIAGEN, Hilden, Germany) according to the manufacturer's protocol, with the final elution volume set at 30 μL. Contaminating genomic DNA was digested with DNase I (Ambion, Austin, TX) at the end of the extraction. Total RNAs from microdissected MPOAs were extracted using an RNAquous®-Micro RNA isolation kit (Ambion), eluted twice with a total volume of 14 μL, and then treated with DNase according to the manufacturer's protocol.

For quantitation of RNA yield, 1 μL of isolated RNA was labeled with a RiboGreen™ RNA Quantitation kit (Molecular Probes, Eugene, Oregon) and concentrations were estimated with a fluorescence spectrophotometer F2500 (Hitachi Co., Tokyo, Japan) in 1 mL of total volume with water.

For microarray analysis, extracted total RNA samples were subjected to amplification, consisting of reverse tran-

scription and subsequent *in vitro* transcription, using a MessageAmp™ aRNA Kit (Ambion) with an oligo dT/T7 primer, according to the manufacturer's protocol. Total RNA samples from liver UFT sections were either subjected to one- or two-step amplification, and those from methacarn-fixed liver PET sections were subjected to two-step amplification. For expression analysis with the microdissected MPOA, two-step amplification was performed. For one-step amplification, 5 μg of total RNA was subjected to one-round of aRNA amplification. For the two-step amplification, 50 ng of total RNA was subjected to first-round amplification, and resultant aRNAs of 150–200 ng were subjected to second-round amplification. During the second *in vitro* transcription, generating aRNAs were labeled with biotin-UTP and biotin-CTP (Enzo Biochem, Farmingdale, NY).

For normalization of transcript levels with reference to amplification efficiency, an *in vitro* transcribed spike RNA from pGIBS-PHE (American Type Culture Collection, Manassas, VA), a short fragment of *Bacillus subtilis* (accession no. M24537 in GenBank/EMBL data bank), was added to the extracted total RNA at 3.76 pg/μg.

After the second-round amplification, 20 μg of biotinylated aRNA was denatured at 94°C for 35 min in fragmentation buffer (4×10^{-2} *M* Tris-acetate, pH 8.1, 1×10^{-7} *M* KOAc, 3×10^{-2} *M* MgOAc) and subjected to hybridization in a mixture containing control cRNAs (Affymetrix, Santa Clara, CA). Aliquots of 200 μL containing approximately 15 μg of aRNA were hybridized with GeneChip® Rat Genome U34A Arrays (Affymetrix) at 45°C for 18 h, stained with streptavidin/R-phycoerythrin conjugates (Molecular Probes), and then scanned with a GeneChip® Scanner 3000 (Affymetrix). Individual samples were subjected to analysis with individual microarrays in both the validation study and the MPOA-specific gene expression profiling study ($n = 3$/group for comparison in each study).

Real-Time RT-PCR

Quantitative real-time RT-PCR was performed for confirmation of expression values obtained with microarrays using ABI Prism 7700 (Applied Biosystems Japan, Tokyo, Japan). In a separate microarray study, to investigate gene expression changes in microdissected MPOA of rat neonates that have been administered 0.01–0.5 ppm ethinylestradiol through the maternal diet, we selected two genes, i.e., thymosin β4 and GTP-binding protein (Gαi2), showing profound sex differences in basal expression. Gene specific primers for thymosin β4 (accession no. NM_031136 in the GenBank/EMBL data banks) and Gαi2 (M12672) as well as corresponding TaqMan® MGB probes (6-FAM™-dye-labeled) were obtained from Assays-on-Demand™ Gene Expression Products (Applied Biosystems Japan). Reverse transcription was performed using 100 ng of first-round aRNAs prepared for microarray analysis containing spike RNA with a high-capacity cDNA Archive Kit (Applied Biosystems Japan) in a 100 μL total reaction volume. Real-time PCR was performed in a 50 μL reaction volume using the TaqMan probe detection system with 25 μL of TaqMan® Universal PCR Master Mix (Applied Biosystems Japan) and 2.5 μL each of target primer mix and RT product. Cycle parameters with this system were: single step of 50°C for 2 min, initial activation at 95°C for 10 min, 45 cycles of 15 sec at 95°C, and 60 sec at 60°C. For quantitation of expression data, a standard curve method was applied using first-round amplified aRNAs from a male MPOA as a standard sample.

For the spike gene (*Bacillus subtilis*), *in vitro* amplified transcript levels were measured by one-step real-time RT-PCR using the SYBR® Green detection system in a 50 μL total reaction mixture containing 25 μL of 2× QuantiTect™ SYBR® Green PCR Master Mix (QIAGEN), 8 ng of first-round amplified aRNA, multiscribe RTase (17.5 units), RNase inhibitor (20 units), and 2.5×10^{-7} *M* of primers. Cycle parameters in this system were as follows: 48°C for 30 min, 95°C for 10 min, 45 cycles of 15 sec at 95°C, and 60 sec at 60°C. The primer set for the spike gene, 5′-AGCGCCCCGGACTGA-3′ (forward; nucleotides 3152–3166), and 5′-CTCTAGGCCCAAAACGACCTT-3′ (reverse; nucleotides 3107–3127), was designed using Primer Express® software (Version 2.0; Applied Biosystems Japan).

Immunohistochemical Analysis

Whole brains of male and female neonates injected with EB or vehicle at PND 1 and obtained on PND 2 were subjected to fixation in Bouin's solution overnight ($n = 4$/sex/group). Coronal brain slices including the hypothalamus were trimmed and paraffin-embedded, and 3-μm serial sections were prepared for localization of the MPOA including the SDN-POA with HE-stained sections each one prepared in every 10 sections.

Immunohistochemistry was performed with antibodies against poly(ADP-ribose) polymerase (PARP) (rabbit IgG, 50× dilution; Santa Cruz Biotechnology, Santa Cruz, CA), glutamate receptor (GluR) 1 (rabbit immunoaffinity purified IgG, 1 μg/mL; Upstate, Charlottesville, VA), GluR5 (rabbit polyclonal IgG, 100× dilution; Upstate), GluR6/7 (rabbit immunoaffinity purified IgG, 5 μg/mL; Upstate), microtubule-associated protein (MAP) 2 (mouse monoclonal IgG_1, 400× dilution; Chemicon International, Inc, Temecula, CA), and metallothionein-1/2 (MT-1/2; clone E9, mouse $IgG_{1\kappa}$, 400× dilution; DakoCytomation, Carpinteria, CA). The PARP antibody can detect PARP-1, and to a lesser extent PARP-2, according to the manufacturer's product information. For detection of GluR1, GluR5, and GluR6/7, deparaffinized sections were subjected to microwave treatment, four times for 3 min in 1×10^{-2} *M* citrate buffer (pH 6.0), according to the recommendation in the manufacturer's protocol. For MAP2, microwave treatment was performed twice for 3 min in the same citrate buffer. Nonspecific endogenous peroxidase activity was blocked by treatment with 0.9% hydrogen peroxide in absolute methanol for 10 min. After masking with normal goat (for rabbit polyclonal antibodies) or horse (for mouse monoclonal antibod-

Table 1 Comparison of the Expression Status of Genes in Microarrays Between aRNA Samples Prepared from UFT and Methacarn-Fixed PET[a]

Tissue Status	UFT		Methacarn-Fixed PET
aRNA Sample	1× amplified	2× amplified	2× amplified
Rates with gene probes for each expression status (%)			
Present	40.3	36.9	36.4
Absent	57.5	60.9	61.5
Marginal	2.2	2.2	2.1
Signal ratio with the GAPDH gene (3′/5′, × fold)	1.1	12.3	11.3

aRNA, antisense RNA; UFT, unfixed frozen tissue; PET, paraffin-embedded tissue; GAPDH, glyceraldehyde-3-phosphate dehydrogenase.
[a] Liver tissue of a rat treated daily with sodium phenobarbital (80 mg/kg body weight, s.c.) for three days was used.

ies) serum, sections were incubated with primary antibodies, overnight at 4°C, and subsequently with biotinylated secondary antibody for 60 min at room temperature. All antibodies used were diluted with 0.5% casein in PBS before application. Immunodetection was carried out with the horseradish peroxidase–avidin–biotin complex utilizing a VECTASTAIN® Elite ABC kit (Vector Laboratories, Burlingame, CA), with 3,3′-diaminobenzidine/H_2O_2 as the chromogen. Sections were counterstained with hematoxylin for microscopic examination. For quantitative measurement of the numbers of nuclei immunoreactive for PARP, bilateral portions of a 250 × 250 μm area covering the SDN region were subjected to analysis under 200× magnification. Also, nuclei immunoreactive for MT-1/2 were counted in bilateral MPOAs by randomly selecting three fields (125 × 125 μm area) on each side under 400× magnification. For each antigen (PARP and MT-1/2), mean ratios of nuclear immunoreactive cells to the total cells counted in each side were estimated.

Data Analysis

Scanned output files of microarrays were visually inspected for hybridization artifacts, and then expression signals for each gene were measured by calculating pixel intensities using a Microarray Suite software package (Version 5.0, Affymetrix). With this software, the expression status of each gene, whether present, absent, or marginally expressed, was judged. Exclusion of genes showing absence in at least three of six samples of the two groups for comparison of expression, normalization of expression data, and statistical comparisons were performed using GeneSpring® software (Version 5; Silicon Genetics; Redwood City, CA). For microarray data in the validation study of expression fidelity with methacarn-fixed PET specimens, per chip normalization was performed by dividing the signal strength for each gene with the level of the 50th percentile of the measurement in the chip, and per gene normalization with average signal strength of the identical gene of three 1×-amplified aRNAs samples from UFTs. With regard to the microarray data for microdissected MPOA, per chip normalization was performed by dividing the signal strength of each gene by the level of the spike RNA signal in each sample, and per gene normalization with average signal strength of the identical gene in three untreated control samples. Average relative expression values were determined for each gene in the treatment group, and genes showing expression changes with ≥2-fold differences were first estimated. Then, comparison of expression data between the untreated controls and each treatment group was performed using Student's *t*-test with multiple testing corrections applying Benjamini and Hochberg false positive discovery rate calculations, and genes showing statistical significance with a p value <0.05 were selected.

To assess fidelity of expression patterns in microarrays between the 2×-amplified aRNA samples from methacarn-fixed liver PETs and 1×- and 2×-amplified samples from liver UFTs, Pearson's correlation coefficients (r) for each combination were estimated using all genes included in the array.

For the real-time RT-PCR data, expression values were normalized to the amplification efficiency of the first-round *in vitro* transcription by dividing the expression values with the signal level of spike RNA included in each sample. Differences in expression levels between sexes were analyzed by the Student's *t*-test, when the variance proved to be homogeneous among groups using the test for equal variance. If a significant difference in the variance was observed, a Welch's *t*-test was performed.

Morphometrically analyzed data for nuclear immunoreactive cell ratios of PARP and MT-1/2 were compared by Student's and Welch's *t*-tests. Regarding immunoreactivities on which morphometric analysis could not be applied, total incidence of immunoreactive cases and grades of intensity were visually analyzed and statistically compared using the Fisher's exact probability test and Mann–Whitney's *U*-test, respectively.

RESULTS

Expression Fidelity in Methacarn-fixed PETs

Expression fidelity of the microdissected small tissue samples in microarray analysis might be influenced by tissue processing for microdissection and/or multiround amplification. To clarify the effect of tissue processing for microdissection (methacarn-fixation and following paraffin-embedding) on the expression

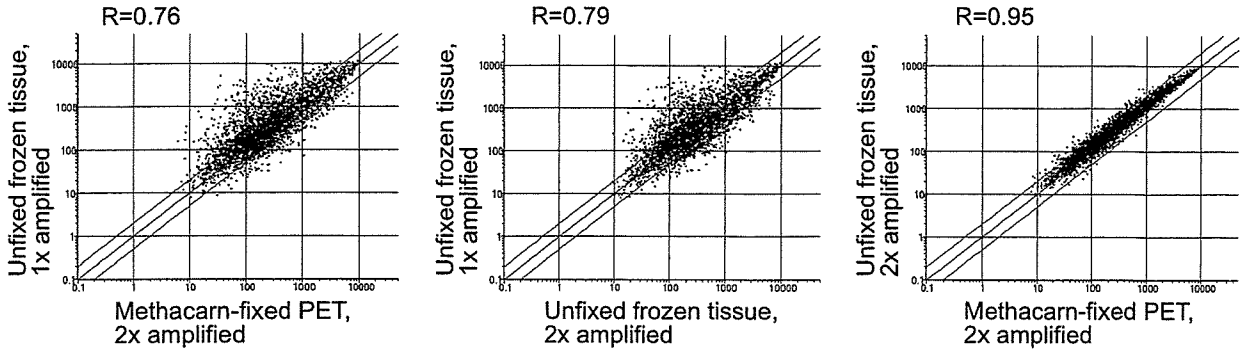

Figure 2 Scatter plot analysis of gene expression profiles of aRNA samples derived from methacarn-fixed PET and UFT of rat liver.

fidelity after 2×-amplification, expression in the second-round amplified aRNA samples was compared with that obtained from the 1×- or 2×-amplified aRNAs from UFT. With the 8799 probes included in the array used, percentages of expression status (present, absent, and marginal) were similar among aRNA-preparations irrespective of the tissue status and the amplification cycle (Table 1). However, preferential amplification of the 3′ portions was evident with 2× amplification in both UFT and methacarn-fixed PET cases (Table 1). By scatter plot analysis, high correlations were observed in the expression profiles between the 2×-amplified aRNAs from methacarn-fixed PET and UFT ($r = 0.95$, $n = 3$; Fig. 2). When the correlation of gene expression levels was examined between the 1×-amplified aRNAs from UFT and 2×-amplified ones from either methacarn-fixed PET or UFT, r values were similar, but relatively low when compared with the value for the correlation between the two 2× amplified examples, indicating a lowered expression fidelity in the methacarn-fixed PET because of the second-round amplification. When the number of genes showing presence was examined for 2×-amplified methacarn-fixed PET and 1×-amplified UFT aRNAs, 3173 probes were positive in common (as shown in Fig. 3). The numbers of probes showing presence solely in the methacarn-fixed PET (2× amplified) and UFT (1× amplified) were 373 and 822, respectively, suggesting that 10.5% of the total genes exhibiting presence in the 2×-amplified samples should be regarded to be false positive, and that 20.6% of the present genes in the 1×-amplified samples from UFT lost their signals after two-round amplification. It is possible that the distance from the poly(A) tail to the positions of the probes may affect the expression status of each gene after the second-round *in vitro* transcription due to preferential amplification of the 3′-terminal portion. Among genes showing presence solely in the methacarn-fixed PET (2× amplified) and UFT (1× amplified), sequence information including the full 3′-untranslated region from the poly(A) tail was available for six and five genes, respectively. The mean distances from the 5′-end of the probes (both 5′- and 3′-most probes) to the 5′-end of poly(A) tail expressed as the number of nucleotides were examined for these (Table 2), and as expected, they were shorter with 2×-amplified aRNA samples from methacarn-fixed PET than with their 1×-amplified counterparts from UFT. These results indicate that the decline in expression fidelity with 2×-amplified samples is mainly due to preferential amplification at the 3′-portions by the second-round amplification and methacarn fixation and paraffin-embedding did not apparently affect the fidelity.

Gene Expression Profiles of MPOA of Neonates Acutely Treated with EB or FA

In the MPOAs at PND 2, about 3600 genes showed presence in both sexes in untreated controls. Sex dif-

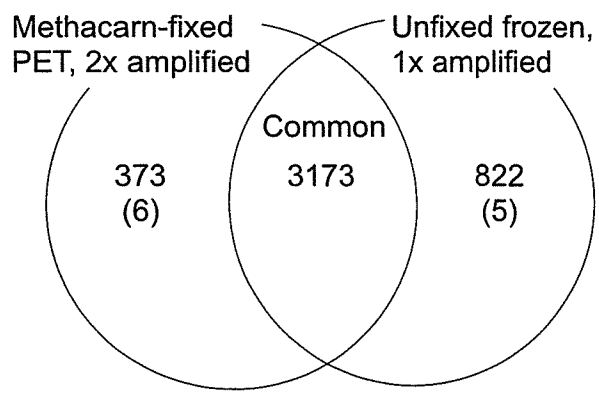

Figure 3 Gene populations showing presence with aRNA samples 2×-amplified from methacarn-fixed PET and 1×-amplified from UFT.

Table 2 Mean Distance from the Probes to the Poly(A) Tail Positions of Genes Showing Presence Solely in the UFT or Methacarn-Fixed PET[a]

aRNA Sample	UFT, 1× amplified	Methacarn-Fixed PET, 2× amplified
Mean distance from the 5′ end of the poly(A) tail (bp)		
No. of genes examined[b]	6	5
3′ end of the 5′ most probe	847	318[c]
3′ end of the 3′ most probe	569	97[c]

aRNA, antisense RNA; UFT, unfixed frozen tissue; PET, paraffin-embedded tissue.

[a] Genes obtained from microarray data in Table 1 were examined.

[b] All genes with sequence information for the 3′-untranslated region were examined.

[c] Significantly different from the unfixed frozen samples ($p < 0.01$).

ferences for male- or female-biased expression were found for 21% and 6% of all present genes, respectively (≥2-fold; Table 3). On EB-treatment, females demonstrated a greater number of genes with expression change. In males, up-regulation by EB was found for only 25 genes, all of them within 2- to 5-fold, and no genes showed down-regulation. In females, up-regulation was detected for a total of 586 genes after EB-treatment (≥2-fold), with 52 genes exhibiting ≥5-fold increase. When compared with up-regulated genes, down-regulated examples were fewer in number in females, with a total of 187 genes showing ≤1/2-fold down-regulation when compared with the vehicle control level. Among them, 33 genes showed ≤1/5-fold down-regulation when compared with vehicle controls. Relatively small numbers of genes showed altered expression on FA-treatment in both sexes. In males, only two and three genes showed up- and down-regulation, respectively (2- to 5-fold change), and in females, three and 22, all of them exhibiting 2- to 5-fold change, except for one gene with ≤1/5-fold up- and down-regulation, respectively.

Among genes showing male-biased expression (≥2-fold difference; 740 genes in total), 59% of them exhibited up-regulation on EB-treatment in females (≥2-fold; 437 genes in total), one of them also exhibiting up-regulation by FA in males (as shown in Fig. 4). One example alone showed down-regulation by FA in males. On the other hand, among genes showing female-biased expression (≥2-fold difference; 203 genes in total), 55% of them exhibited down-regulation by EB in females (≤1/2-fold; 111 genes in total). Among them, a total of 10 genes also showed altered expression by FA; nine genes down-regulated in females and one gene up-regulated in males. On the other hand, five female-predominant genes exhibited up-regulation by EB in males, four of them also showing down-regulation by EB in females, with one gene each further showing down-regulation in females and up-regulation in males by FA-treatment.

When genes that demonstrated changed expression levels in both sexes by the chemical treatments were examined, four genes encoding the LINE retrotransposable element 3, L1Rn B6 repetitive DNA element, ADP-ribosyltransferase (adprt) 1, and NonO/p54nrb homolog, exhibited up-regulation in males and down-regulation in females by EB-treatment and also female-biased expression (Table 4). Expression levels for genes showing male-biased expression were not affected by EB. FA-treatment did not alter the expression level of any gene involving both sexes.

Table 5 shows the list of genes showing altered expression in the MPOA of either sex common to both chemicals. Among the total of 15, 12 showed down-regulation in females common to EB and FA, eight of them exhibiting female-biased expression, i.e., for protein tyrosine phosphatase, receptor type, F (*PTPRF*); DAP-like kinase (*dlk*); glutamate receptor, kainate receptor subunit (KA1); dyskeratosis congenita 1 (*dyskerin*); L1Rn B6 repetitive DNA element; *MAP2*; expressed sequence tag (EST), similar to the mouse estrogen-responsive finger protein (*efp*); and glutamate receptor, ionotropic, AMPA subtype (GluR1).

Table 3 Number of Genes Showing Sex Differences in Basal Expression as well as Alteration After EB or FA Treatment in the Neonatal MPOA ($p < 0.05$)

Difference/Change (× fold)	2–5	≥5
Sex difference		
Males > females	676	64
Females > males	176	27
Altered by EB		
Males		
Up-regulated	25	0
Down-regulated	0	0
Females		
Up-regulated	534	52
Down-regulated	154	33
Altered by FA		
Males		
Up-regulated	2	0
Down-regulated	3	0
Females		
Up-regulated	3	0
Down-regulated	22	0

EB, estradiol benzoate; FA, flutamide; MPOA, medial preoptic area.

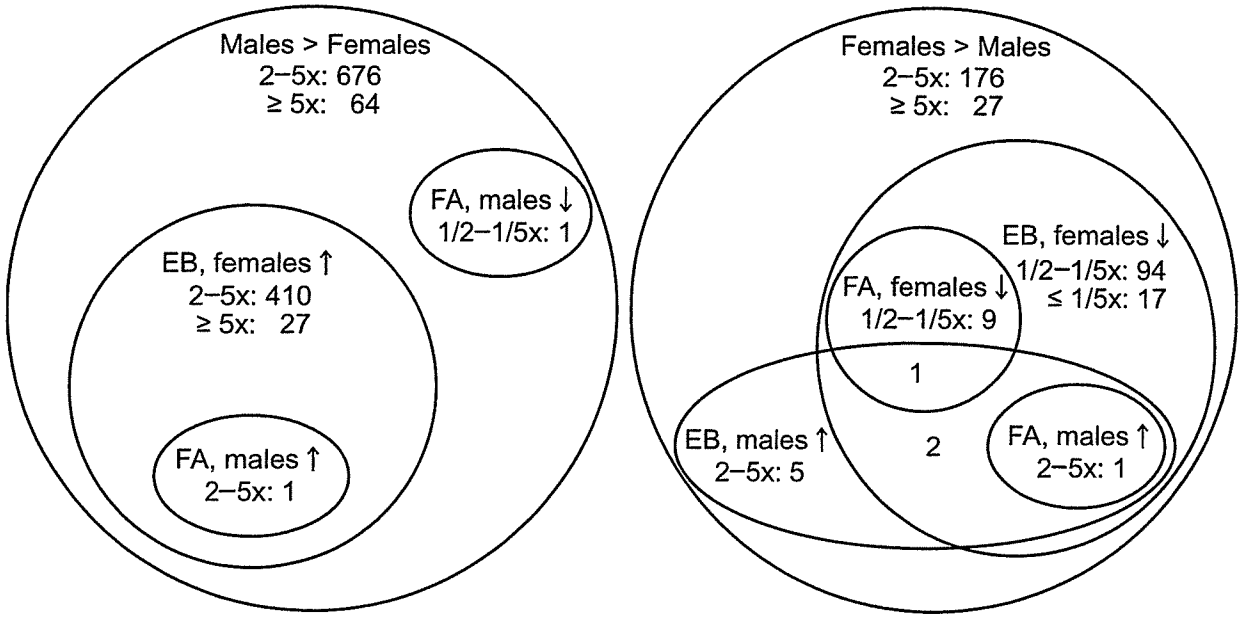

Figure 4 Distribution of gene populations showing altered expression with EB and/or FA-treatment among those showing sex differences in expression in the neonatal MPOA.

Interestingly, two subtypes of glutamate receptors, KA1 and GluR1, exhibited this particular expression pattern, the former being detected with two different probe sets (accession nos. U08257 and X59996). Without showing sex differences in the basal expression, expression of five genes were influenced by EB and FA, the following four exhibiting down-regulation in females with both chemicals: myeloid/lymphoid or mixed-lineage leukemia (trithorax (drosophila) homolog); translocated to, 3; cyclin D1; serine/threonine kinase 25; and neurotrimin. On the other hand, one EST (accession no. AI639097) showed up-regulation by EB and down-regulation by FA in females. Among the genes listed in Table 5, up-regulated examples were rather few and the magnitude of up-regulation was within 2- to 3-fold. In addition to the altered expression involving both sexes after EB treatment (see above), two genes showed altered expression with FA, i.e., down-regulation of the L1Rn B6 repetitive DNA element in females, and up-regulation of the LINE retrotransposable element 3 in males. Among those showing male-biased expression, there was only one with altered expression due to both EB and FA. MT1a transcripts showed up-regulation by EB in females and also by FA in males.

Fig. 5 shows mRNA expression data for two genes by real-time RT-PCR regarding sex differences in the neonatal MPOAs observed with microarrays. Both thymosin $\beta 4$ and $G\alpha i2$ mRNAs exhibited strong male-biased expression at PND 2, with 8.9- and 7.1-fold higher levels than in females. Real-time RT-PCR results confirmed this sex difference.

Immunoreactivity of Protein Signals

Fig. 6 shows representative figures for immunohistochemical demonstration of protein signals in the MPOA with the anatomical location indicated in

Table 4 List of Genes Showing Altered Expression in the MPOA of Both Sexes by EB-Treatment (≥2-fold, $p < 0.05$)

			Altered by EB (× fold *vs.* control)	
Accession No.	Gene	Sex Difference (× fold)	M	F
M13100	LINE retrotransposable element 3	M<F (2.9)	2.1	0.5
X07686	L1Rn B6 repetitive DNA element	M<F (3.8)	2.0	0.4
AA964849	ADP-ribosyltransferase (adprt) 1	M<F (3.3)	2.2	0.3
AF036335	NonO/p54nrb homolog	M<F (5.5)	3.2	<0.1

MPOA, medial preoptic area; EB, estradiol benzoate; FA, flutamide; M, males; F, females; EST, expressed sequence tag.

Table 5 List of Genes Showing Altered Expression in the MPOA Common to EB and FA (≥2-fold, $p < 0.05$)

Accession No.	Gene	Sex Difference (× fold)	Altered by EB (× fold *vs.* control)		Altered by FA (× fold *vs.* control)	
			M	F	M	F
M13100	LINE retrotransposable element 3	M<F (2.9)	2.1	0.5	2.2	–
U87960	Protein tyrosine phosphatase, receptor type, F (PTPRF); leukocyte common antigen receptor (LAR)	M<F (11.8)	–	0.1	–	0.4
AJ006971	DAP-like kinase (dlk)	M<F (6.4)	–	0.3	–	0.3
U08257 (X59996)	Glutamate receptor, ionotropic, kainite 4 (Grik4); Kainate receptor subunit (KA1)	M<F (5.8) (M<F (5.4))	– (–)	0.3 (0.2)	– (–)	0.5 (0.5)
AA892562	Dyskeratosis congenita 1, dyskerin (dkc1)	M<F (4.0)	–	0.4	–	0.4
X07686	L1Rn B6 repetitive DNA element	M<F (3.8)	2.0	0.4	–	0.2
X53455	Microtubule-associated protein 2 (MAP2)	M<F (3.5)	–	0.1	–	0.3
AA859593	EST, similar to mouse estrogen-responsive finger protein (efp)	M<F (3.4)	–	0.3	–	0.5
X17184	Glutamate receptor, ionotropic, AMPA subtype, GluR1	M<F (3.1)	–	0.3	–	0.5
AJ006295	Myeloid/lymphoid or mixed-lineage leukemia (trithorax (Drosophila) homolog); translocated to, 3 (mllt3); AF-9	–	–	0.4	–	0.5
AI231257	Cyclin D1	–	–	0.4	–	0.5
AA799791	Serine/threonine kinase 25 (STE20 homolog, yeast) (stk25)	–	–	0.4	–	0.4
U16845	Neurotrimin	–	–	0.5	–	0.5
AI639097	EST	–	–	2.2	–	0.5
AI176456	Metallothionein (MT1a)	M>F (2.8)	–	2.9	2.3	–

MPOA, medial preoptic area; EB, estradiol benzoate; FA, flutamide; M, males; F, females; EST, expressed sequence tag.

Figure 1. In the hypothalamus at PND 2, nuclear immunoreactivity of PARP, the protein product of the *adprt* gene (Skaper, 2003), was observed in the ventricular ependymal and subependymal cells around the third ventricle. On quantitative measurement of nuclear immunoreactivity at the SDN region, cases with higher grades of distribution were more frequent in female controls when compared with the males [Figs. 6(A,B) and 7]. EB-treatment increased and decreased the positive cell distribution in males and females, respectively [Figs. 6(C) and 7]. GluR1 immunoreactivity was observed in the cytoplasm and dendritic processes of neuronal cells, its staining intensity being mostly weak in the MPOAs, even in the positive cases, when compared with the other brain areas, such as the hippocampus, cerebral cortex, and striatum [Fig. 6(D)]. In the MPOAs of male controls, two out of four cases showed only minimal intensity of GluR1-immunoreactivity, and the other two showed negative results [Fig. 6(D), Table 6]. Although the intensity was minimal to slight, all control females showed positive immunoreactivity in their MPOAs [Fig. 6(E)]. EB-treatment did not alter the intensity in either sex [female: Fig. 6(F)]. With regard to GluR5, very faint immunoreactivity was observed in the dendritic processes in the striatum and bed nucleus, but staining was lacking in the MPOAs of both sexes, even with the EB treatment

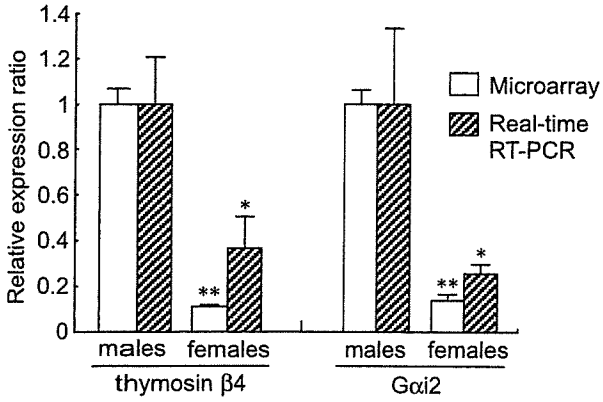

Figure 5 Confirmation of microarray data by real-time RT-PCR in the neonatal MPOA. Sex differences in the mRNA expression of thymosin $\beta 4$ and Gαi2 were analyzed. Significantly different from the male value in each detection system ($*p < 0.05$, $**p < 0.01$).

(Table 6). GluR6/7-immunoreactivity was observed in the cytoplasm of both neuronal and glial cells of the whole brain area, but there was no obvious change in terms of the distribution and intensity in the MPOAs, irrespective of the sex or EB treatment (Table 6). MAP2 immunoreactivity was observed in the whole dendritic processes with a fibrillary expression pattern, but there was no obvious change in terms of the distribution and intensity in the MPOAs, irrespective of the sex or EB treatment (Table 6). Strong cytoplasmic immunoreactivity of MT-1/2 was observed in the astrocytes located in the deep cortex and white matter of the cerebrum, hippocampal white matter, and striatum [Fig. 6(G)]. In other brain areas, MT-1/2-immunoreactivity was rather weak and sparse, and both nuclear and cytoplasmic. In the MPOAs, nuclear immunoreactivity predominated over cytoplasmic staining. On quantitative measurement of the nuclear immunoreactivity, the positive cell ratio was higher in males than in females, with increase in the latter on EB treatment [Figs. 6(G–I) and 7].

DISCUSSION

In the present validation study to establish a region-specific microarray analysis method using PET samples in combination with methacarn fixation, we found that gene expression profiles were very similar between 2×-amplified aRNAs from UFT and methacarn-fixed PET, and the deviation in expression data with the second-round amplification from the 1×-amplified aRNAs of UFT was mostly due to the preferential amplification of the 3′-terminal portion, irrespective of the tissue status. These results strongly indicate that methacarn fixation and subsequent paraffin embedding do not affect the expression fidelity in microarray analyses. Although it is still necessary to improve expression fidelity with second-round amplification, the results suggest an advantage of methacarn in combination with paraffin embedding for global gene expression analysis of microdissected cellular regions. It should be stressed that paraffin embedding is essential for preparation of serial sections necessary for microdissection of anatomically defined tissue areas.

Although the sex difference in the incidence of apoptosis in the SDN region that is believed to be re-

Figure 6 Immunoexpression patterns for PARP (panels A-C), GluR1 (panels D-F), and MT-1/2 (panels G-I), in the neonatal rat MPOA at PND 2. A. Note scattered PARP-immunoreactive nuclei (arrowheads) in paraventricular cells of a control male. The inset shows a high-power view of the nuclear weak immunoreactivity in the same area. B. Distribution of PARP-weakly immunoreactive cell nuclei in a control female. Note accumulation of positive cells in the SDN region (arrow). C. Lack of PARP-immunoreactive cells in most paraventricular and SDN regions in an EB-treated female. D. Very weak, mostly negative GluR1-immunoreactivity in the cytoplasmic processes of neurons in a control male. The inset shows strong immunoreactivity in the cytoplasm and dendritic processes of neuronal cells of the cerebral cortex of the same brain section. E. Slight intensity of GluR1-immunoreactivity in cytoplasmic processes of neurons in a control female. The inset shows a high-power view of the immunoreactivity in cytoplasmic processes of the same area. F. Minimal degree of GluR1-immunoreactivity in an EB-treated female. G. Diffuse immunoexpression of MT-1/2 in a control male. The expression pattern is mostly nuclear, and both astrocytic (arrowheads) and neuronal (arrows) populations as well as ependymal cells (*) show apparent immunoreactivity. The inset shows strong expression in cytoplasmic processes of astrocytes in the deep cerebral cortex of the same brain section. H. Scattered weak nuclear immunoreactivity of MT-1/2 in a control female. I. Diffuse nuclear and scattered cytoplasmic distribution of immunoreactive cells in an EB-treated female. The inset shows a high power view of both nuclear and cytoplasmic immunoreactivity in the same area. Bar = 50 μm, including insets.

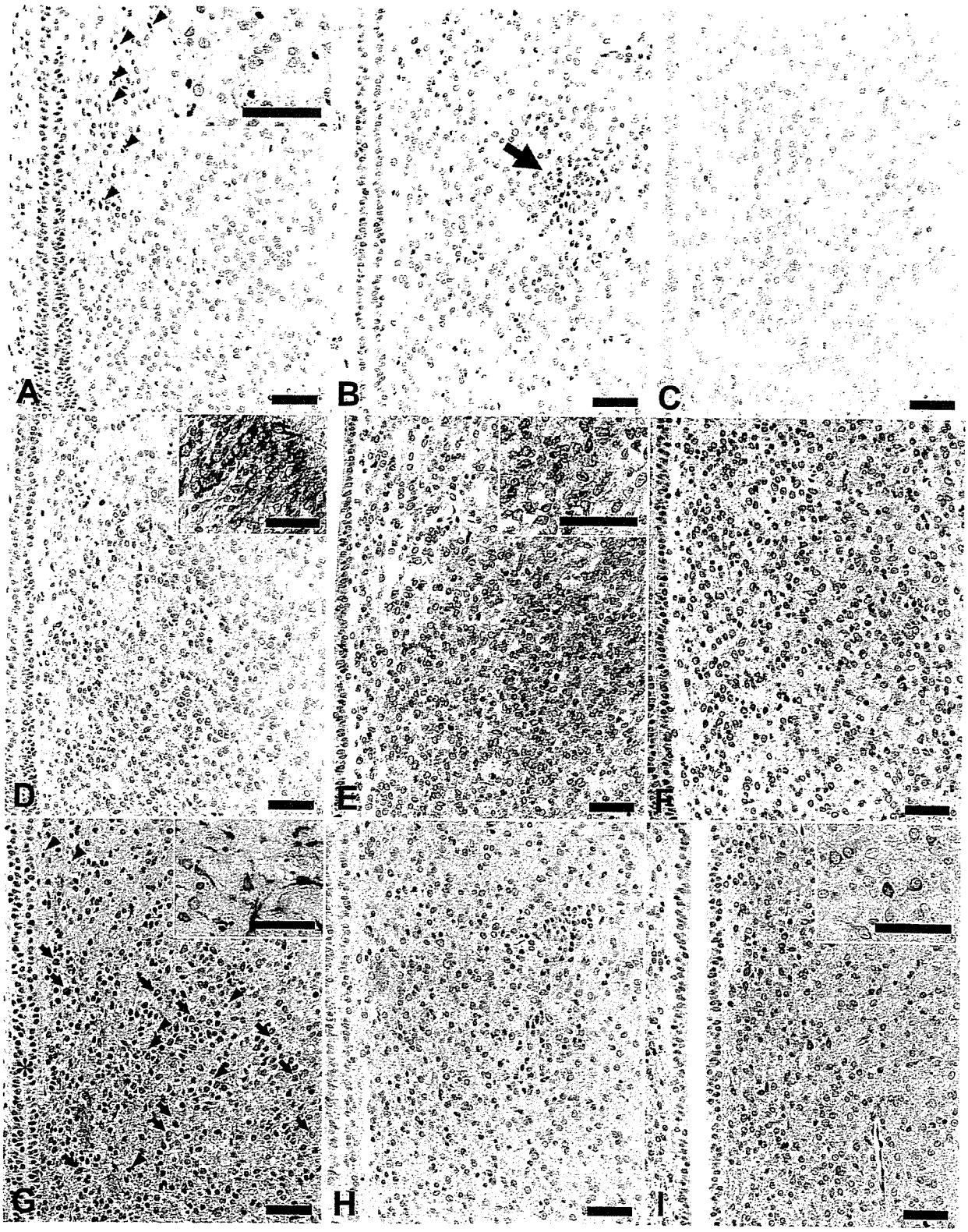

Figure 6

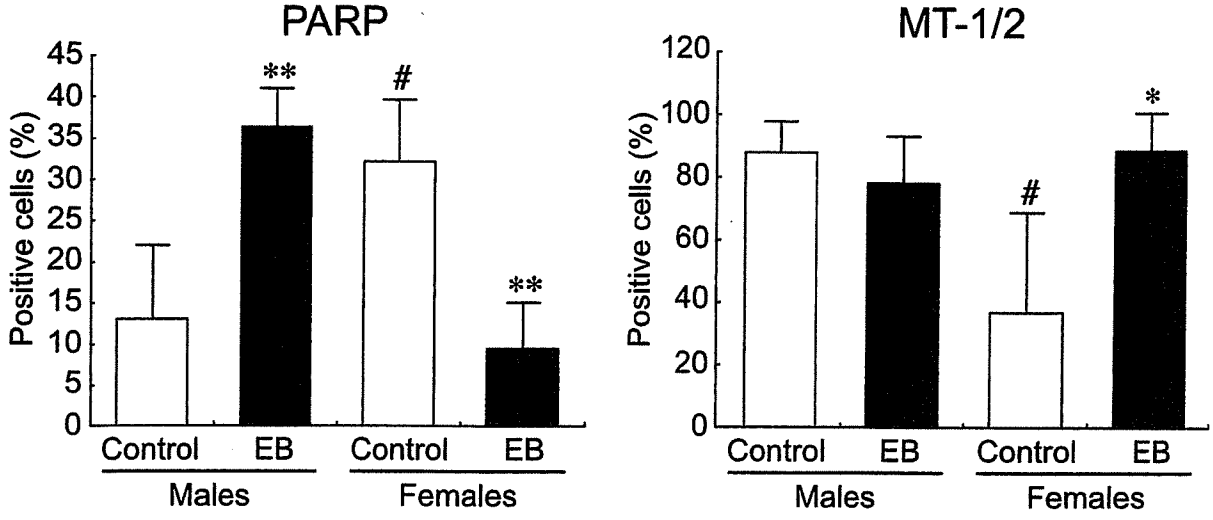

Figure 7 Nuclear immunoreactive cell percentages for PARP and MT-1/2 in neonatal rat MPOAs at PND 2. Significantly different from the corresponding controls ($^{*}p < 0.05$, $^{**}p < 0.01$). Significantly different from the male controls ($^{\#}p < 0.05$).

sponsible for subsequent sexually dimorphic development of this nucleus first occurs between PNDs seven and 10 (Davis et al., 1996), the number of genes exhibiting male-biased constitutive expression was much higher than in females at time points as early as PND 2 in the present study. This sex difference is presumably the reflection of growth and/or antiapoptotic effects for male-type large SDN under the influence of estradiol generated by aromatase from testosterone perinatally secreted from the developing testis (Matsumoto et al., 2000). Regarding responses to chemicals, the number of genes showing altered expression by EB or FA was far greater in females than in males, suggesting an effect on normal female sexual differentiation. Moreover, approximately 60% of genes showing male or female-biased expression demonstrated altered levels with EB in females, pointing to an involvement of genes necessary for normal processes of male- or female-type brain sexual differentiation in its disruptive effects. It is well known that the perinatal/neonatal treatment of animals with estrogenic compounds can affect sexual development of both sexes, resulting in reproductive dysfunction (Nagao et al., 1999; Odum et al., 2002; Tsukahara et al., 2003; Shibutani et al., 2005). With regard to the effects of antiandrogens, disruption of sexual development has generally been apparent in males, but the situation is largely unclear for females (Gray and Kelce, 1996; Wolf et al., 2004). With FA, however, prenatal exposure affects the volume of the anteroventral periventricular nucleus (AVPVN) in female rats (Lund et al., 2000) and the female sexual behavior in guinea pigs (Thornton et al., 1991). In addition, FA exerts antiprogestin activity (Chandrasekhar and Armstrong, 1989; Dukes et al., 2000).

Our search for genes showing altered expression by EB or FA revealed a total of four female-predominant genes with change by EB in both sexes, all up-regulated in males and down-regulated in females. Two of them are long interspersed repetitive DNAs, L1, or LINE, a class of mobile genetic elements named retrotransposons which can be amplified by retroposition, i.e. by a mechanism similar to that observed with retroviruses (Servomaa and Rytoamaa,

Table 6 Immunoreactivity of Protein Signals in the MPOA of Neonatal Rats Treated with EB[a]

	Males		Females	
Antigen	Control	EB	Control	EB
Number of animals	4	4	4	4
GluR1 (±/+)[b]	2[c](2/0)[d]	3(3/0)	4(3/1)	3(3/0)
GluR5 (present)	0	0	0	0
GluR6/7 (±/+/++)[b]	4(2/2/0)	4(0/4/0)	4(0/3/1)	4(2/2/0)
MAP2 (±/+/++)[b]	4(0/3/1)	4(0/3/1)	4(2/2/0)	4(2/2/0)

Protein signals with immunoexpression patterns for which morphometric analysis could not be applied were analyzed by visual estimation of the grade of intensity of immunoreactivity in the MPOA. MPOA, medial preoptic area; EB, estradiol benzoate; GluR1, glutamate receptor 1; GluR5, glutamate receptor 5; GluR6/7; glutamate receptor 6/7; MAP2, microtubule-associated protein 2.

[a] Rat neonates treated with EB at 10 μg/pup or vehicle on PND1 and sacrificed 24 h later were examined.

[b] Grades of intensity of immunoreactivity: ±, minimal; +, slight; ++, moderate; and +++, prominent.

[c] Total number of animals showing positive immunoreactivity.

[d] Number of animals with each grade.

1990). This group of retrotransposons includes regulatory signals and encodes two proteins, a RNA-binding protein and an integrase-replicase (Han and Boeke, 2005). The human genome contains about 500,000 LINES, accounting for roughly 17% of the total (Haoudi et al., 2004). Various environmental factors, such as steroid hormone-like agents and stressors can facilitate L1 transcription to alter cellular functions (Servomaa and Rytoamaa, 1990; Morales et al., 2002, 2003). Moreover, a regulatory role of L1 repeats at the promoter region has been reported with estrogen-related gene transcription (Hardy et al., 2001). During neuronal differentiation, retrotransposition events can alter the expression of neuronal genes, which, in turn, can influence neuronal cell fate (Muotri et al., 2005). Thus, the sex differences in the retrotransposon expression in the developing MPOA apparent here suggest roles in sex-dependent gene expression control, and alteration in their expression status due to EB may indicate roles as upstream regulators of genes necessary for brain sexual differentiation.

Two other genes showing up-regulation in males and down-regulation in females with EB, as well as female-biased expression, were *adprtl* and *NonO/p54nrb*. *Adprtl* encodes PARP-1, an abundant nuclear enzyme that is activated primarily by DNA damage; however, its excessive activation can lead to cell death (Skaper, 2003; Koh et al., 2005). Interestingly, sex differences exist regarding PARP-1 activation as well as nitric oxide toxicity in a mouse ischemic neurotoxicity model (McCullough et al., 2005). In the periventricular cell populations, poly(ADP-ribosyl)ation is basally activated by DNA strand breaks reflecting glutamate-nitric oxide neurotransmission (Pieper et al., 2000). In the present study, the measured level of PARP-immunoexpression at the SDN region was in line with the microarray data, suggesting an induction of subsequent programmed cell death in the female SDN-POA (Davis et al., 1996). Similarly, increased expression of PARP in males and its decrease in females with EB here may be linked to the decreased SDN volume in males in later life (Shibutani et al., 2005) and the decreased apoptosis in the female SDN after EB injection (Arai et al., 1996), respectively. NonO/p54nrb has been implicated in a variety of nuclear processes (Proteau et al., 2005). Indeed, this protein is known to act as a transcription factor necessary for adrenocortical steroidogenesis (Sewer et al., 2002), and as a transcriptional co-activator of the human androgen receptor (AR; Ishitani et al., 2003).

In the present study, a total of 15 genes exhibited altered expression due to FA in either sex, in addition to alteration by EB. Among them, 10 genes also exhibited sex differences in expression including the two genes for retrotransposons mentioned earlier. Interestingly, many of the 15 genes exhibited similar expression patterns with EB and FA, most being down-regulated in females, suggesting a common mechanism of action of the two chemicals. The following seven genes showed this particular expression pattern, in addition to the L1 repeat mentioned earlier: *PTPRF*/leukocyte common antigen-related (LAR) protein, *dlk*, two kinds of glutamate receptors, *dyskerin*, *MAP2*, and *efp*. In males, neonatal estrogen treatment affects the developing testis to suppress androgen secretion, presumably resulting in effects similar to antiandrogenicity on postnatal development (Atanassova et al., 1999). On the other hand, FA in the 20-day pubertal female assay using rats has been shown to exert ER-agonist activity on female sexual development, attributed to an imbalance between endogenous estrogenic and androgenic stimuli in the target organs (Kim et al., 2002).

Regarding glutamate receptors, mRNA expression of GluR1, the AMPA subtype found here with altered expression, is up-regulated in the AVPVN by estrogen in ovariectomized juvenile female rats (Gu et al., 1999). Hypothalamic GluR1 protein level was also increased in gonadectomized and estrogen-treated adult rats irrespective of the sex (Diano et al., 1997). Different from our female neonates, these results suggest that estrogen could up-regulate GluR1 levels in the juvenile/adult rat hypothalamus, probably through a different mechanism from that during sexual differentiation. In the female MPOA, we here could detect a slight, but nonsignificant increase in GluR1-immunoreactive cases when compared with those in males. Although we could not examine immunohistochemical localization of KA1 subunit here, other kainate receptor subtypes (GluR5, 6, and 7) have shown, in a study using adult rats, to be expressed in tanycytes, astrocytes, and neurons of the arcuate nucleus, with co-expression of AR or ER found in neurons in males and females, respectively (Diano et al., 1998). However, we could not detect any sex difference or EB-induced effect on the immunoreactivity of GluR5 or GluR6/7 in the neonatal MPOA.

PTPRF/LAR is a widely expressed tyrosine phosphatase that has been implicated in the regulation of a diverse range of signaling pathways, such as in the development and maintenance of excitatory synapses, and interestingly, disruption of its function results in reduction of surface AMPA receptors (Mooney and LeVea, 2003; Dunah et al., 2005). In the present study, AMPA subtype GluR1, as mentioned earlier, showed similar responses to EB and FA as well as a sex differ-

ence in mRNA expression, suggesting a coordinated action of PTPRF/LAR and AMPA receptors during brain sexual differentiation and its disruption.

MAP2 contributes to regulation of cytoskeletal organization and dynamics, and is expressed mainly in dendritic processes of neurons (Maccioni and Cambiazo, 1995). Posttranscriptional control of MAP2 expression has been reported in the female rat hippocampus in response to estrogen treatment or during the estrous cycle (Reyna-Neyra et al., 2002, 2004). Interestingly, estrogen can induce dendrite spines in the developing rat POA through activation of AMPA-kainate receptors by glutamate that may originate from astrocytes (Amateau and McCarthy, 2002). Inconsistent with the microarray data, MAP2-immunoreactivity in the neonatal MPOA here lacked any sex difference or change in expression on chemical treatment as in the case with above-mentioned GluR5 and GluR6/7.

Efp, a target gene product of ERα, is a RING-finger-dependent ubiquitin ligase that targets proteolysis of 14-3-3σ, a negative cell cycle regulator that causes G2 arrest (Urano et al., 2002), and is considered essential for estrogen-dependent tumor cell proliferation (Horie et al., 2003). This gene product is distributed mainly in estrogen-sensitive organs/tissues associated with ER co-expression (Orimo et al., 1995; Shimada et al., 2004). Dlk is a nuclear serine/threonine-specific kinase that has been implicated in the regulation of apoptosis by relocation to the cytoplasm, but its nuclear location has been suggestive of the roles for mitosis and cytokinesis (Preuss et al., 2003). Dyskerin, a nucleolar protein that modifies specific uridine residues of rRNA, also acting as a component of the telomerase complex, is a target molecule for skin and bone marrow failure syndrome called dyskeratosis congenita in human (Marrone et al., 2005). Dyskerin transcripts distribute ubiquitously in embryo-fetal tissues with notably high levels in epithelial and neural tissues (Heiss et al., 2000).

As a unique gene showing male-biased expression and increase with EB in females and decrease with FA in males, *MT1a* is of interest. MTs are considered to be important metal-binding proteins active in defense against heavy metal toxicity (Sogawa et al., 2001), and four major MT isoforms have so far been identified. In the present study, judging from the sequence information (accession no. AI176456) for the MT probes, either MT1 or 2 was suggested to be responsible for the particular expression pattern. Sex steroid-related expression changes in MT1 and/or 2 have been reported in the liver or brain of mice (Sogawa et al., 2001; Beltramini et al., 2004). In the brain, MT1 and 2 are expressed mainly in nonneuronal cells (Suzuki et al., 1994; Hidalgo et al., 2001), but certain levels are also found in neurons (Xie et al., 2004); as well as cytoplasmic expression, nuclear localization of MT has been reported in developing brain (Suzuki et al., 1994). Interestingly, kainic acid treatment can selectively induce MT1 in neurons and MT2 in glial cells in rats (Kim et al., 2003). Although the immunoreactivity of MT-1/2 was rather weak when compared with other brain areas and a nuclear expression was predominant in the neonatal MPOA here, male predominance may reflect a neuroprotective function, and expression changes due to EB and FA could indicate alteration in the regional hormonal environment in response to treatment.

In summary, we here established the basis for a global gene expression profiling method using paraffin-embedded, histologically defined small tissue areas with methacarn as a fixative. A male predominance in the number of genes showing constitutively higher expression suggestive of sex steroidal effects on the neonatal male MPOA was detected. Upon treatment with EB, many genes showing sex differences in expression demonstrated altered levels in females, in line with involvement of genes necessary for brain sexual differentiation in its disruption. Moreover, many genes commonly affected by EB and FA showed down-regulation in females with these drugs, suggesting common mechanisms shared between estrogenic and anti-androgenic chemicals in induction of endocrine center disruption in females, at least in early stages.

We thank Mrs. Keiko Kuroiwa for her technical assistance in conducting the immunohistochemical study. Dr. Lee was an Awardee of a Postdoctoral Fellowship from the Japan Society for the Promotion of Science during the performance of the study.

REFERENCES

Amateau SK, McCarthy MM. 2002. A novel mechanism of dendritic spine plasticity involving estradiol induction of prostaglandin-E_2. J Neurosci 22:8586–8596.

Arai Y, Sekine Y, Murakami S. 1996. Estrogen and apoptosis in the developing sexually dimorphic preoptic area in female rats. Neurosci Res 25:403–407.

Atanassova N, McKinnell C, Walker M, Turner KJ, Fisher JS, Morley M, Millar MR, et al. 1999. Permanent effects of neonatal estrogen exposure in rats on reproductive hormone levels, Sertoli cell number, and the efficiency of spermatogenesis in adulthood. Endocrinology 140:5364–5373.

Beltramini M, Zambenedetti P, Wittkowski W, Zatta P. 2004. Effects of steroid hormones on the Zn, Cu and MTI/II levels in the mouse brain. Brain Res 1013:134–141.

Chandrasekhar Y, Armstrong DT. 1989. Ability of progesterone to reverse anti-androgen (hydroxyflutamide)-induced interference with the preovulatory LH surge and ovulation in PMSG-primed immature rats. J Reprod Fertil 85:309–316.

Davis EC, Popper P, Gorski RA. 1996. The role of apoptosis in sexual differentiation of the rat sexually dimorphic nucleus of the preoptic area. Brain Res 734:10–18.

Diano S, Naftolin F, Horvath TL. 1997. Gonadal steroids target AMPA glutamate receptor-containing neurons in the rat hypothalamus, septum and amygdala: A morphological and biochemical study. Endocrinology 138:778–789.

Diano S, Naftolin F, Horvath TL. 1998. Kainate glutamate receptors (GluR5-7) in the rat arcuate nucleus: Relationship to tanycytes, astrocytes, neurons and gonadal steroid receptors. J Neuroendocrinol 10:239–247.

Dukes M, Furr BJ, Hughes LR, Tucker H, Woodburn JR. 2000. Nonsteroidal progestins and antiprogestins related to flutamide. Steroids 65:725–731.

Dunah AW, Hueske E, Wyszynski M, Hoogenraad CC, Jaworski J, Pak DT, Simonetta A, et al. 2005. LAR receptor protein tyrosine phosphatases in the development and maintenance of excitatory synapses. Nat Neurosci 8:458–467.

Gray LE Jr, Kelce WR. 1996. Latent effects of pesticides and toxic substances on sexual differentiation of rodents. Toxicol Ind Health 12:515–531.

Gu G, Varoqueaux F, Simerly RB. 1999. Hormonal regulation of glutamate receptor gene expression in the anteroventral periventricular nucleus of the hypothalamus. J Neurosci 19:3213–3222.

Han JS, Boeke JD. 2005. LINE-1 retrotransposons: Modulators of quantity and quality of mammalian gene expression? Bioessays 27:775–784.

Haoudi A, Semmes OJ, Mason JM, Cannon RE. 2004. Retrotransposition-competent human LINE-1 induces apoptosis in cancer cells with intact p53. J Biomed Biotechnol 2004:185–194.

Hardy DO, Niu EM, Catterall JF. 2001. Kap promoter analysis *in vivo*: A regulatory role for a truncated L1 repeat. Mol Cell Endocrinol 181:57–67.

Heiss NS, Bächner D, Salowsky R, Kolb A, Kioschis P, Poustka A. 2000. Gene structure and expression of the mouse dyskeratosis congenita gene, *dkc1*. Genomics 67: 153–163.

Hidalgo J, Aschner M, Zatta P, Vasak M. 2001. Roles of the metallothionein family of proteins in the central nervous system. Brain Res Bull 55:133–145.

Horie K, Urano T, Ikeda K, Inoue S. 2003. Estrogen-responsive RING finger protein controls breast cancer growth. J Steroid Biochem Mol Biol 85:101–104.

Ishitani K, Yoshida T, Kitagawa H, Ohta H, Nozawa S, Kato S. 2003. p54nrb acts as a transcriptional coactivator for activation function 1 of the human androgen receptor. Biochem Biophys Res Commun 306:660–665.

Kim D, Kim EH, Kim C, Sun W, Kim HJ, Uhm CS, Park SH, et al. 2003. Differential regulation of metallothionein-I, II, and III mRNA expression in the rat brain following kainic acid treatment. Neuroreport 14:679–682.

Kim HS, Shin JH, Moon HJ, Kim TS, Kang IH, Seok JH, Kim IY, et al. 2002. Evaluation of the 20-day pubertal female assay in Sprague-Dawley rats treated with DES, tamoxifen, testosterone, and flutamide. Toxicol Sci 67: 52–62.

Kocarek TA, Kraniak JM, Reddy AB. 1998. Regulation of rat hepatic cytochrome P450 expression by sterol biosynthesis inhibition: Inhibitors of squalene synthase are potent inducers of CYP2B expression in primary cultured rat hepatocytes and rat liver. Mol Pharmacol 54:474–484.

Koh DW, Dawson TM, Dawson VL. 2005. Poly(ADP-ribosyl)ation regulation of life and death in the nervous system. Cell Mol Life Sci 62:760–768.

Lund TD, Salyer DL, Fleming DE, Lephart ED. 2000. Pre or postnatal testosterone and flutamide effects on sexually dimorphic nuclei of the rat hypothalamus. Brain Res Dev Brain Res 120:261–266.

Maccioni RB, Cambiazo V. 1995. Role of microtubule-associated proteins in the control of microtubule assembly. Physiol Rev 75:835–864.

Marrone A, Walne A, Dokal I. 2005. Dyskeratosis congenita: Telomerase, telomeres and anticipation. Curr Opin Genet Dev 15:249–257.

Masutomi N, Shibutani M, Takagi H, Uneyama C, Takahashi N, Hirose M. 2003. Impact of dietary exposure to methoxychlor, genistein, or diisononyl phthalate during the perinatal period on the development of the rat endocrine/reproductive systems in later life. Toxicology 192: 149–170.

Matsumoto A, Sekine Y, Murakami S, Arai Y. 2000. Sexual differentiation of neuronal circuitry in the hypothalamus. In: Matsumoto A, editor. Sexual Differentiation of the Brain. Boca Raton: CRC Press, pp 203–227.

McCullough LD, Zeng Z, Blizzard KK, Debchoudhury I, Hurn PD. 2005. Ischemic nitric oxide and poly (ADP-ribose) polymerase-1 in cerebral ischemia: Male toxicity, female protection. J Cereb Blood Flow Metab 25:502–512.

McEwen BS, Alves SE. 1999. Estrogen actions in the central nervous system. Endocr Rev 20:279–307.

Meisel RL, Sachs BD. 1994. The physiology of male sexual behavior. In: Knobil E, Neills JD, editors. The Physiology of Reproduction, 2nd ed. New York: Raven Press, pp 3–106.

Meredith JM, Bennett C, Scallet AC. 2001. A practical three-dimensional reconstruction method to measure the volume of the sexually-dimorphic central nucleus of the medial preoptic area (MPOC) of the rat hypothalamus. J Neurosci Methods 104:113–121.

Mooney RA, LeVea CM. 2003. The leukocyte common antigen-related protein LAR: Candidate PTP for inhibitory targeting. Curr Top Med Chem 3:809–819.

Morales JF, Snow ET, Murnane JP. 2002. Environmental factors affecting transcription of the human L1 retrotransposon. I. Steroid hormone-like agents. Mutagenesis 17:193–200.

Morales JF, Snow ET, Murnane JP. 2003. Environmental factors affecting transcription of the human L1 retrotransposon. II. Stressors. Mutagenesis 18:151–158.